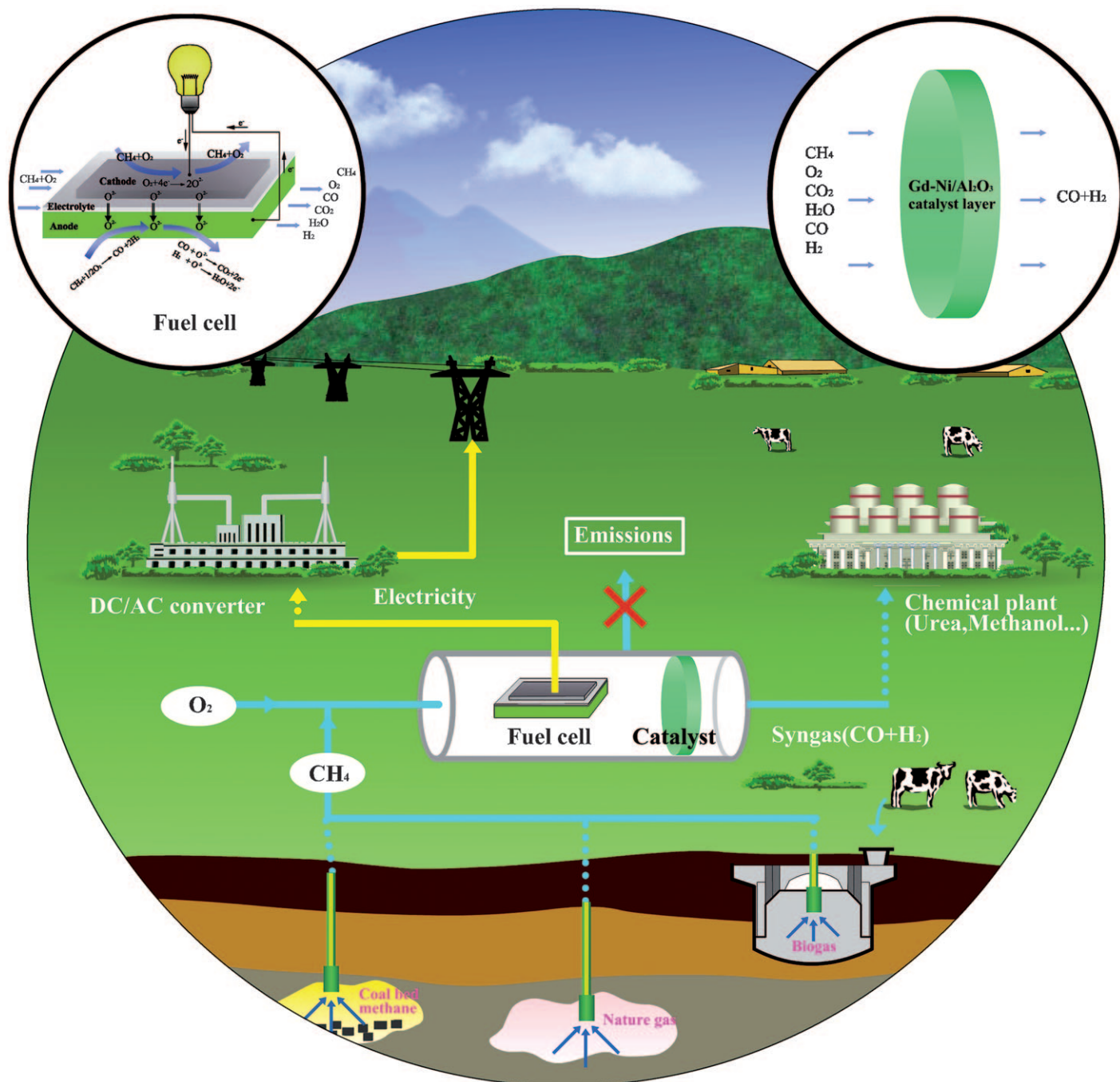


# Electric Power and Synthesis Gas Co-generation From Methane with Zero Waste Gas Emission\*\*

Zongping Shao,\* Chunming Zhang, Wei Wang, Chao Su, Wei Zhou, Zhonghua Zhu, Hee Jung Park, and Chan Kwak



Solid-oxide fuel cells (SOFCs) are energy converters with a high energy efficiency and low environmental impact.<sup>[1]</sup> SOFCs could be more cost-effective when they are simultaneously operated as chemical reactors to produce useful chemicals.<sup>[2]</sup> Co-generation of electric power and synthesis gas from methane could be realized in two SOFC configurations, namely conventional dual-chamber<sup>[3]</sup> and more simplified sealant-free single-chamber SOFCs (SC-SOFCs).<sup>[4]</sup> However, there is a trade-off between high power and simple system configuration between the two configurations; furthermore, synthesis gas formation rate and methane conversion are strongly influenced by polarization current in both configurations. Herein we show that these issues can be circumvented by integrating a downstream catalyst in the same gas chamber of a single-chamber SOFC. A bilayer electrolyte fuel cell achieved an open-circuit voltage of 1.07 V and a maximum peak power density of about 1500 mW cm<sup>-2</sup> at 700 °C operating on methane–oxygen gas mixture with a ratio of 2:1. By passing the effluent gas of the fuel cell through a GdNi/Al<sub>2</sub>O<sub>3</sub> catalyst at 850 °C, the synthesis gas is obtained with a methane conversion of higher than 95 %, CO and H<sub>2</sub> selectivity higher than 98 %, and a H<sub>2</sub>/CO ratio of about two. We also show that both the synthesis gas formation rate and H<sub>2</sub> and CO molar ratio are unaffected by the polarization current density. By enabling conversion of the abundant resources of methane to synthesis gas and electricity without releasing any waste gases, the system has great potential to make significant contributions to the low-carbon economy.

Methane can be catalytically converted into synthesis gas by partial oxidation ( $\text{CH}_4 + 1/2 \text{O}_2 \rightarrow \text{CO} + 2\text{H}_2$ )<sup>[5]</sup> or be applied as a fuel for a SOFC for electric power generation.<sup>[6,7]</sup> The partial oxidation reaction is mildly exothermic ( $\Delta H_{298\text{K}} = -36 \text{ kJ mol}^{-1}$ ), which means some of the enthalpy of methane is wasted by thermal heat during the synthesis gas formation process. Furthermore, the heat released during the fast reaction may be accumulated, resulting in a substantial temperature increment in the catalyst layer, thereby introducing a serious safety problem.<sup>[8]</sup> On the other hand, by

applying methane as a fuel for the fuel cell for power generation alone, there is still at least 40 % of enthalpy wasted by thermal heat, along with the production of CO<sub>2</sub> greenhouse gas. By co-generation of electricity and synthesis gas from methane, an overall efficiency up to 100 % and also improved operational safety may be realized.

Conventional fuel cells have a dual-chamber configuration for electricity and synthesis gas co-generation; pure methane is fed to the anode chamber and oxygen for the partial oxidation is transported from the cathode.<sup>[3,9]</sup> The synthesis gas formation rate and methane conversion are all strongly influenced by the polarization current.<sup>[3]</sup> Furthermore, coke is easily formed over the nickel-based cermet anode, especially under a low polarization current density. A previous study showed that the electric power and synthesis gas cogeneration can also be realized in a SC-SOFC using a Pt|electrolyte|Au fuel cell assembly.<sup>[4]</sup> However, an extremely low power density was reached owing to the low catalytic activity of the Au cathode, and the conversion of methane was also inevitably influenced by the polarization current. Herein, a SC-SOFC integrated with a GdNi/Al<sub>2</sub>O<sub>3</sub> partial oxidation catalyst in the same gas chamber was applied for the facile co-generation of electricity and synthesis gas from methane with zero waste gas emission (Figure 1). By applying a methane–oxygen mixture (CH<sub>4</sub>/O<sub>2</sub> molar ratio 2:1) as the feed gas, high cell power output, high methane conversion, high H<sub>2</sub> and CO selectivities, and an ideal H<sub>2</sub> to CO molar ratio of about two for Fischer–Tropsch fuel and methanol synthesis could be reached.

SC-SOFC, with both its electrodes exposing to the same fuel/oxidant gas mixture in a mono gas chamber, is a novel type of SOFC.<sup>[10]</sup> Its operation principle relies on the different catalytic activity and selectivity of the electrodes towards the fuel/oxidant mixture. Previously, Shao and Haile have shown that Ba<sub>0.5</sub>Sr<sub>0.5</sub>Co<sub>0.8</sub>Fe<sub>0.8</sub>O<sub>3-δ</sub> (BSCF) is a promising cathode for SC-SOFCs, with a high electrocatalytic activity for oxygen reduction but poor catalytic activity for hydrocarbon oxidation.<sup>[11,12]</sup> However, the fuel cell suffers from a low open-circuit voltage (OCV) of 0.70–0.78 V,<sup>[13]</sup> which is mainly due to the partial electronic conductivity of the samarium-doped ceria (SDC) electrolyte at elevated temperatures.<sup>[14]</sup> Although the electron conduction in SDC is obviously suppressed with the drop of operation temperature, an increase in OCV is not envisioned because of insufficient catalytic activity of anode for methane partial oxidation.

We adopt an anode-supported fuel cell with 8 mol % yttrium-stabilized zirconia (YSZ) and SDC bilayer electrolyte to reduce partial electron conduction and avoid the interfacial reaction between YSZ and BSCF. The fuel cell is operated at elevated temperature to increase the electrode activity and stability under a CO<sub>2</sub>-containing atmosphere. We fabricate the fuel cell by a facile technique based on tape casting the anode layer, spray depositing and co-sintering the YSZ and SDC electrolyte layers, and screen printing the cathode layer. The bilayer electrolyte has a clear layer boundary, and the porous Ni + YSZ cermet anode (Ni/YSZ = 60:40 by weight) and BSCF + SDC cathode (BSCF/SDC = 70:30 by weight) adhere well to the YSZ and SDC layers, respectively (Supporting Information, Figure S1).

[\*] Prof. Z. P. Shao, C. M. Zhang, W. Wang, C. Su  
 State Key Laboratory of Materials-Oriented Chemical Engineering  
 Nanjing University of Technology  
 Nanjing, 210009 (PR China)  
 Fax: (+86) 25-8317-2256  
 E-mail: shaozp@njut.edu.cn

Dr. W. Zhou, Prof. Z. H. Zhu  
 School of Chemical Engineering, The University of Queensland  
 Brisbane, Queensland 4072 (Australia)

Dr. H. J. Park, Dr. C. Kwak  
 Samsung Advanced Institute of Technology (SAIT)  
 14-1 Nongseo-dong, Yongin-si, 446-712 (Korea)

[\*\*] This work was supported by the National Science Foundation for Distinguished Young Scholars of China under contract No. 51025209, the National Basic Research Program of China under contract No. 2007CB209704, by the Outstanding Young Scholar Grant at Jiangsu Province under contract No. 2008023, by the program for New Century Excellent Talents (2008), and by the Fok Ying Tung Education Foundation under contract No. 111073.

Supporting information for this article is available on the WWW under <http://dx.doi.org/10.1002/anie.201006855>.

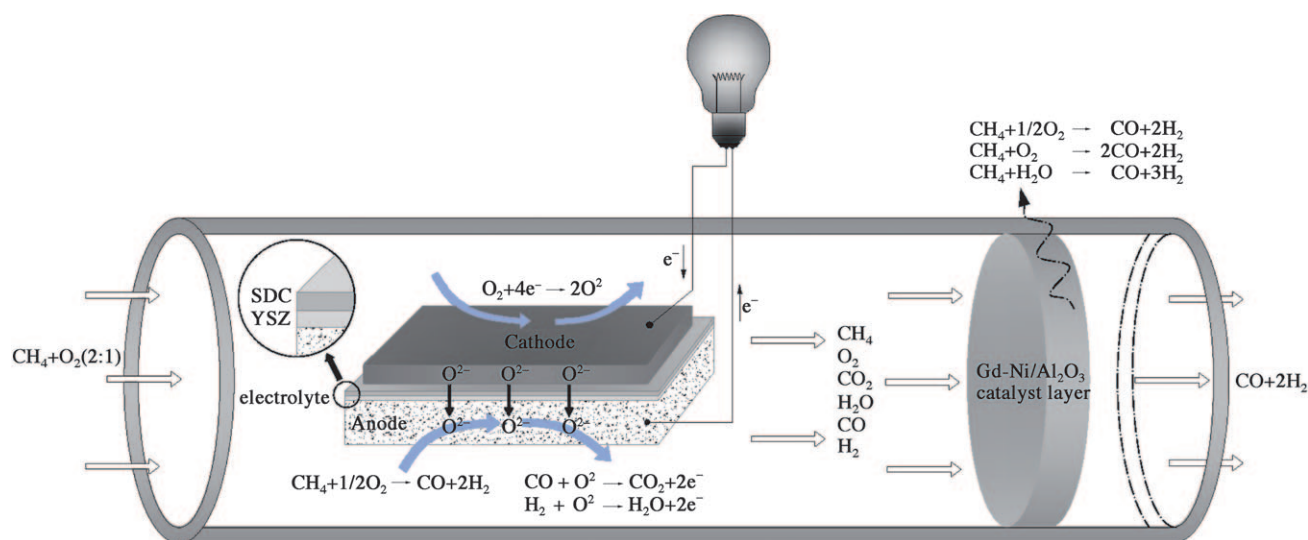


**Figure 1.** The fuel cell reactor system used for synthesis gas and electric power co-generation from methane. The fuel cell and the GdNi/Al<sub>2</sub>O<sub>3</sub> catalyst were located in a single quartz tube reactor ( $\varnothing = 14$  mm and  $L = 300$  mm). The feed gas was composed of methane and oxygen at the molar ratio of 2:1, which was introduced from one side of the reactor, first passed through the fuel cell, and then the catalyst layer. Both the fuel cell and catalyst were heated up by electric furnaces.

We first measured the current–voltage and current–power polarization curves of the fuel cell operating on a methane–oxygen gas mixture with molar ratio of 2:1 at furnace temperatures of between 550 and 700 °C (Figure 2). Under open-circuit conditions, the cell voltage is 1.05–1.07 V, significantly improved compared to a similar cell with a single SDC electrolyte of 0.70–0.78 V operating on a methane–helium–oxygen mixture gas.<sup>[13]</sup> By applying the bilayer electrolyte, electron diffusion in the electrolyte is effectively blocked. On the other hand, the oxygen partial pressure at the cathode side is improved by applying a methane–oxygen mixture as the feed gas ( $P_{\text{O}_2} = 0.33$  atm) instead of a methane–

oxygen–helium mixture ( $P_{\text{O}_2} = 0.18$  atm). At a furnace temperature of 700 °C, a peak power density of about 1500 mW cm<sup>−2</sup> is achieved for a cell with 5 μm YSZ and 5 μm SDC bilayer electrolytes. The peak power density still reaches 1200 mW cm<sup>−2</sup> for a cell with a 10 μm YSZ and 5 μm SDC bilayer electrolyte (Supporting Information, Figure S2), which is comparable to about 1260 mW cm<sup>−2</sup> for a similar cell operating at 850 °C in a dual chamber configuration by applying the same methane–oxygen gas mixture as the anode gas and air as the oxidant (Supporting Information, Figure S3), and substantially higher than the results reported for conventional SC-SOFCs (Supporting Information, Table 1).<sup>[10–13, 15–19]</sup> It is also much higher than the value of 400 mW cm<sup>−2</sup> for a similar anode-supported SC-SOFC with a single YSZ electrolyte and the same BSCF + SDC cathode (Figure 3).

The catalytic activity of the Ni + YSZ cermet anode for the methane partial oxidation reaction (Figure 3) was tested in a flow-through type fixed-bed quartz-tube reactor with an inner diameter of about 8 mm. Catalyst particles (ca. 0.1 g) in the size range of 40–60 mesh were placed into middle of the reactor. The compositional analysis was conducted by a Varian 3800 gas chromatograph equipped with the Hayesep Q, Poraplot Q and 5 Å sieve molecular capillary columns and a TCD for the separation and detection of H<sub>2</sub>, O<sub>2</sub>, CO, CO<sub>2</sub>, and CH<sub>4</sub>.

The performance of a SC-SOFC operating on a methane–oxygen gas mixture is closely related to the electrocatalytic activity of the cathode for oxygen reduction and catalytic activity of the anode for methane partial oxidation. Area-specific resistance (ASR) is as low as 0.011 Ω cm<sup>−2</sup> at 800 °C for the BSCF electrode on a SDC electrolyte operating on a methane–oxygen gas mixture, as determined by a symmetric cell test (Supporting Information, Figure S4). As for the anode, the methane partial oxidation not only creates a low

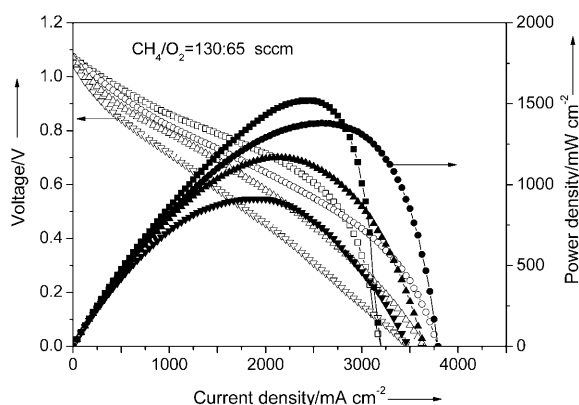


**Figure 2.** Performance of a bilayer electrolyte fuel cell operating on a CH<sub>4</sub>/O<sub>2</sub> gas mixture. The cell voltage and power output are presented as functions of current density at different temperatures (□ 700 °C, ○ 650 °C, △ 600 °C, ▽ 550 °C). Data were obtained in single-chamber mode from a single cell composed of BSCF + SDC cathode (BSCF/SDC = 70:30 by weight, ca. 20 μm), SDC (ca. 5 μm) and YSZ (ca. 5 μm) bilayer electrolyte, and Ni + YSZ anode (NiO/YSZ = 60:40 by weight, ca. 700 μm). Total flow rate: 195 mL min<sup>−1</sup> (STP), cathode surface area: 0.48 cm<sup>2</sup>.

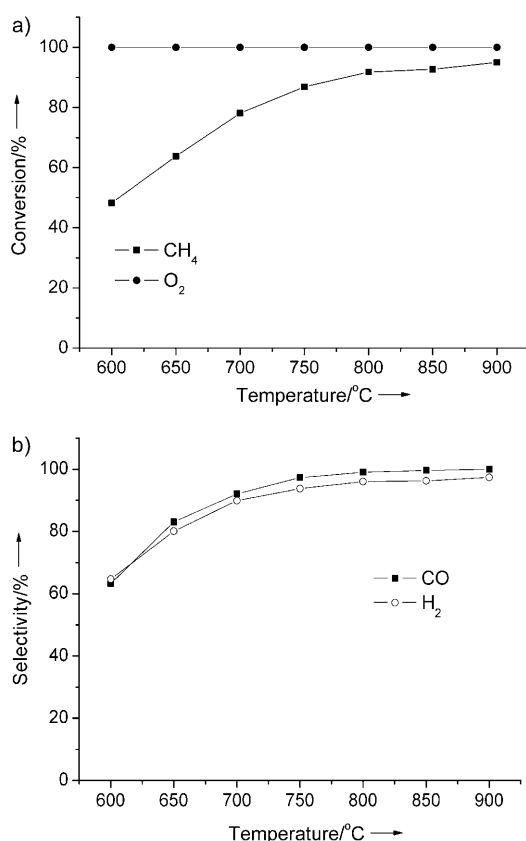


**Figure 3.** The catalytic activity of the Ni + YSZ cermet anode for the methane partial oxidation reaction. a) Conversion as a function of temperature: ■ CH<sub>4</sub>, ● O<sub>2</sub>. b) Selectivity: ■ CO, ○ O<sub>2</sub>. Methane flow rate: 20 mL min<sup>-1</sup> (STP), CH<sub>4</sub>/O<sub>2</sub> 2:1; helium was used as diluting gas with a flow rate of 80 mL min<sup>-1</sup> (STP).

oxygen potential near the anode surface, which is critical to increase the oxygen potential differential across the two electrodes, but also produces electrochemically active H<sub>2</sub> and CO species as the direct fuels for power generation. Catalytic tests show that the oxygen was completely converted at temperatures higher than 600 °C, while CO and H<sub>2</sub> selectivities reach about 80 % at 700 °C by applying a sintered anode powder as a catalyst (Supporting Information, Figure S5). Because of the exothermic nature of the methane partial oxidation, the real temperature of a SC-SOFC is 110–150 °C higher than the furnace (Supporting Information, Figure S6). Thus, the conventional Ni + YSZ cermet anode performs well as a partial oxidation catalyst at the furnace temperatures of 600–700 °C. Both the high electrocatalytic activity of the BSCF + SDC cathode for oxygen reduction and the catalytic activity of the Ni-YSZ cermet anode for methane partial oxidation then leads to the high cell performance.

One practical problem associated with BSCF cathode is its high sensitivity to CO<sub>2</sub> poisoning. A serious deterioration in electrocatalytic activity for oxygen reduction was reported with the presence of unavoidable CO<sub>2</sub> at reduced temperatures<sup>[20]</sup> in a SC-SOFC. A symmetric cell with BSCF electrodes and a SDC electrolyte was first investigated by electrochemical impedance spectroscopy (EIS) in air, then

5 % CO<sub>2</sub> was introduced into the atmosphere and EIS of the cell at different operation times were recorded. Figure 4 shows the corresponding EIS in Nyquist plots at 600–800 °C. The poisoning effect of CO<sub>2</sub> on the BSCF electrode is significantly decreased with increasing operation temperature. Specifically, at a cell temperature of 800 °C, 5 % CO<sub>2</sub> in the air atmosphere has an almost negligible effect on the oxygen reduction behavior of the BSCF. The slightly larger EIS of the cell under 5 % CO<sub>2</sub>-containing air than that under pure air is due to the diluting effect of the oxygen by CO<sub>2</sub>. Thus the operation at elevated temperature contributes an additional benefit for improving the operational stability of SC-SOFCs.

Because of the poor activity of the BSCF + SDC cathode for methane partial oxidation,<sup>[13]</sup> a considerable amount of methane is unconverted alongside the production of large amounts of deep oxidation products of CO<sub>2</sub> and H<sub>2</sub>O in the effluent gas of the fuel cell (Figure 5). By adopting a combustion-synthesized GdNi/Al<sub>2</sub>O<sub>3</sub> catalyst in the downstream of the fuel cell, which has been shown to have high catalytic activity for methane partial oxidation, steam reforming, and CO<sub>2</sub> reforming at temperatures higher than 700 °C (Supporting Information, Figure S7), a substantial increase in methane conversion and H<sub>2</sub> and CO selectivities was observed. A methane conversion of more than 95 % and a H<sub>2</sub>/CO ratio of about 2.0 were reached at temperature of 850 °C for the catalyst layer (Figure 6). No obvious change in methane conversion, H<sub>2</sub> and CO selectivities, and the H<sub>2</sub>/CO ratio was observed by varying the polarization current (Supporting Information, Table S2), which is a significant advantage for practical applications. The result can be well understood by considering the fixed O<sub>2</sub> to CH<sub>4</sub> ratio in the feed gas. By first converting partial chemical energy stored in methane into electric power, the following synthesis gas formation reaction over the GdNi/Al<sub>2</sub>O<sub>3</sub> catalyst becomes milder, and consequently the problem of temperature runaway that occurs for the methane partial oxidation can be effectively avoided by optimizing the operation parameters. Although the efficiency of a SC-SOFC is lower than the conventional dual-chamber SOFC, by transferring partial enthalpy of methane into the synthesis gas, it is possible to make the whole system have 100 % fuel efficiency. The above results thus promise the co-generation of electric power and synthesis gas from methane by SC-SOFC technology for the full utilization of methane with zero greenhouse gas emission.

### Experimental Section

**Fuel cell fabrication:** Anode substrates were prepared by a tape-casting process. The slurry for tape-casting process was prepared by two-step ball milling. Commercial nickel oxide (Chengdu Shudu Nanomaterials Technology Development Co. Ltd.), YSZ (Tosoh) and starch were ball milled together with organic solvent in an agate jar for 24 h. Triethanolamine was added as surfactant for the dispersion of oxide powder in organic solvent in the first step. In the second step, polyvinyl butyral (PVB) as binder, polyethylene glycol (PEG), and dibutyl *o*-phthalate (DOP) as plasticizer were added to the slurry and then ball milled again for another 24 h. The slurry was vacuum pumped under 200 mbar (absolute pressure) to remove air and then cast onto the polymer carrier on a tape-casting machine. The slurry



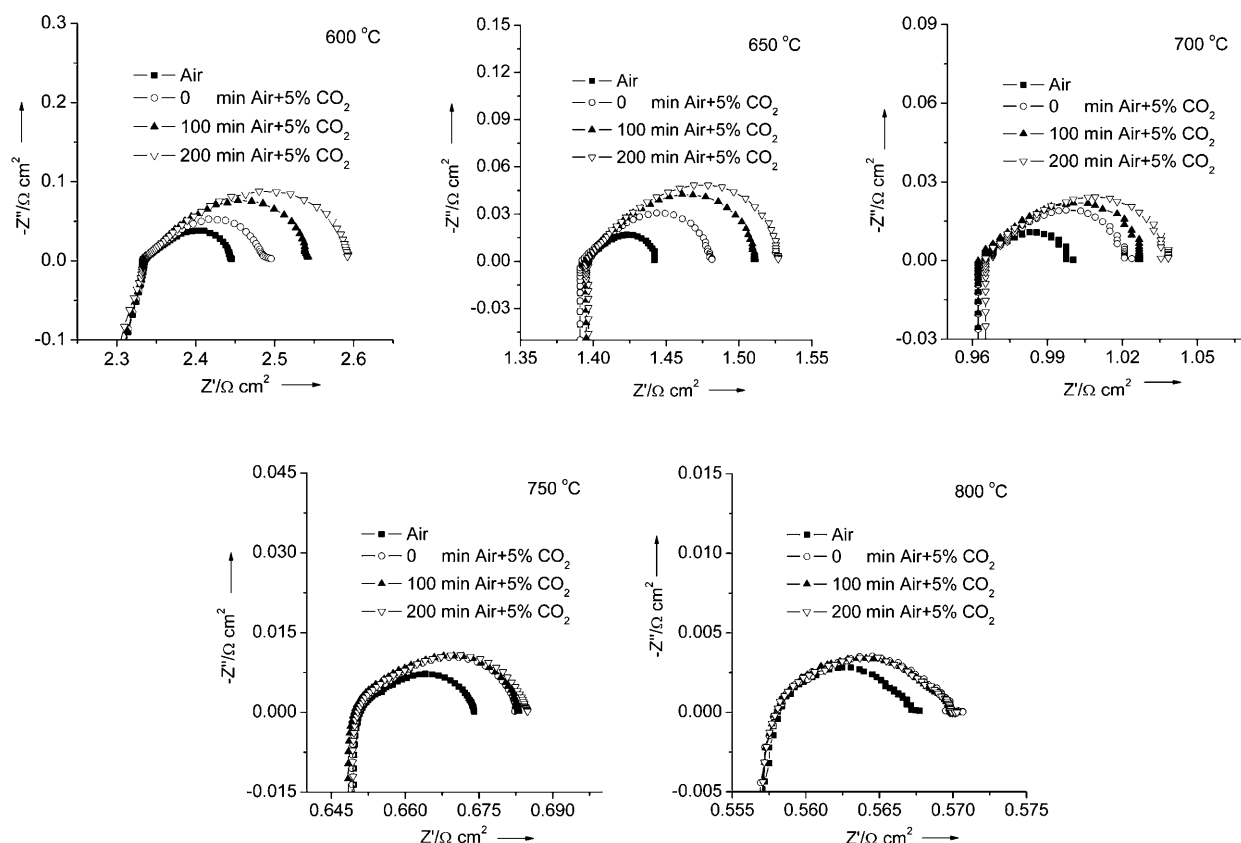


**Figure 4.** The effect of CO<sub>2</sub> on the activity of the BSCF + SDC electrode for oxygen electrochemical reduction at various temperatures. The test was made by measuring the area-specific resistances (ASRs) of the BSCF + SDC electrode in a symmetric cell configuration. The cell was first tested in a synthetic air atmosphere (O<sub>2</sub> + N<sub>2</sub>, P<sub>O<sub>2</sub></sub> = 0.21 atm), then 5 % CO<sub>2</sub> was introduced, and the ASRs were measured periodically. Flow rate of the mixture gas: 157.5 mL min<sup>-1</sup> (STP); electrode surface area: about 1.2 cm<sup>2</sup>.

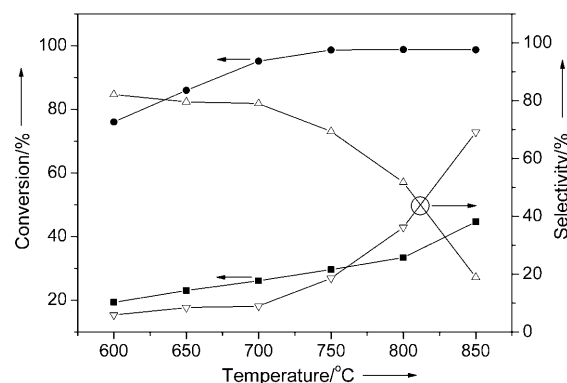


**Figure 5.** CH<sub>4</sub>/O<sub>2</sub> conversion (■ CH<sub>4</sub>, ● O<sub>2</sub>) and CO/CO<sub>2</sub> selectivity (Δ CO<sub>2</sub>, ▽ CO) as a function of temperature for the methane oxidation reaction under normal single-chamber operation conditions. CH<sub>4</sub>/O<sub>2</sub> 2:1, total flow rate 195 mL min<sup>-1</sup> (STP). The effluent gas was introduced to a gas chromatograph (Varian 3800) equipped with the Haysep Q, Poraplot Q, and 5 Å molecular sieve capillary columns and a thermal conductivity detector (TCD).

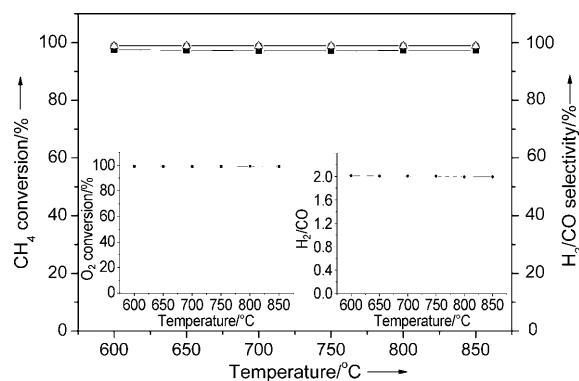


**Figure 6.** Gas composition and H<sub>2</sub>/CO ratios of the effluent gas from a SC-SOFC operating on methane–oxygen gas mixture after passing through the GdNi–Al<sub>2</sub>O<sub>3</sub> catalyst layer at 850 °C. ■ CH<sub>4</sub>, ○ H<sub>2</sub>, Δ CO. Inserts: oxygen conversion and the corresponding H<sub>2</sub>/CO ratios at different temperatures.

was dried in air for 24 h and then detached from the tape. Anode substrates for single cells were drilled from the NiO + YSZ tape with a diameter of 16 mm. The disks were then sintered at elevated temperature for subsequent electrolyte deposition.

The YSZ electrolyte layer and SDC interlayer were prepared by a wet powder-spraying technique. The YSZ and SDC powders were prepared into colloidal suspensions with solid content of about 5 %. The colloidal suspension was then sprayed under the drive of 1 atm nitrogen carrier gas onto the anode substrate (or YSZ) using a modified spraying gun (BD-128, Fenghua Bida Machinery Manufacture Co. Ltd., China) with a nozzle size of 0.35 mm (pore diameter).

The spray gun was aligned above the heated substrate (250 °C on a hot plate) at a distance of 10 mm. The calculated effective deposition speed was about 0.005–0.008 g cm<sup>-2</sup> min<sup>-1</sup> YSZ/SDC. The cells were then sintered at 1400–1500 °C for 5 h in air. BSCF + SDC (7:3 w/w) was applied as the cathode, which was screen-printed on the central surface of the electrolyte and fired at 1000 °C in air for 2 h to allow the firm attachment of the cathode layer onto the electrolyte (interlayer) surface. The coin-shaped cathode had an effective area of 0.48 cm<sup>2</sup>.

The GdNi/Al<sub>2</sub>O<sub>3</sub> catalyst with the composition of 5.56 wt % Gd<sub>2</sub>O<sub>3</sub>, 15 wt % nickel, and 79.44 wt % Al<sub>2</sub>O<sub>3</sub> was synthesized by a glycine nitrate process (GNP). Stoichiometric amounts of nickel nitrate (2.55 mol), gadolinium nitrate (0.31 mol), and alumina nitrate (1.56 mol) were first dissolved in deionized water, and then glycine as a fuel was added at a molar ratio of 2.0 between the glycine and total metallic cations. The water in the solution was evaporated by heating over a hot plate at 80 °C under stirring to create a gel precursor, which was moved to an electrical oven at 240 °C to trigger the autocombustion. The primary powder obtained was further calcined at 850 °C for 5 h in static air to yield the desired catalyst.

Received: November 2, 2010

Published online: February 3, 2011

**Keywords:** electrochemistry · fuel cells · heterogeneous catalysis · methane · synthesis gas

- [1] B. C. H. Steele, A. Heinzl, *Nature* **2001**, *414*, 345–352.  
 [2] F. Alcaide, P. Cabot, E. Brillas, *J. Power Sources* **2006**, *153*, 47–60.

- [3] T. Ishihara, T. Yamada, T. Akbay, Y. Takita, *Chem. Eng. Sci.* **1999**, *54*, 1535–1540.  
 [4] T. Hibino, H. Iwahara, *Chem. Lett.* **1993**, 1131–1134.  
 [5] D. A. Hickman, L. D. Schmidt, *Science* **1993**, *259*, 343–346.  
 [6] S. Park, J. M. Vohs, R. J. Gorte, *Nature* **2000**, *404*, 265–267.  
 [7] E. Perry, T. Tsai, S. A. Barnett, *Nature* **1999**, *400*, 649–651.  
 [8] K. Nakagawa, N. Ikenagam, T. Kobayashi, T. Suzuki, *Catal. Today* **2001**, *64*, 31–41.  
 [9] T. Tagawa, K. K. Moe, M. Ito, S. Goto, *Chem. Eng. Sci.* **1999**, *54*, 1553–1557.  
 [10] T. Hibino, A. Hashimoto, T. Inoue, J. Tokuno, S. Yoshida, M. Sano, *Science* **2000**, *288*, 2031–2033.  
 [11] Z. P. Shao, S. M. Haile, *Nature* **2004**, *431*, 170–173.  
 [12] Z. P. Shao, S. M. Haile, J. Ahn, P. D. Ronney, Z. L. Zhan, S. A. Barnett, *Nature* **2005**, *435*, 795–798.  
 [13] Z. P. Shao, J. Mederos, W. C. Cheuh, S. M. Haile, *J. Power Sources* **2006**, *162*, 589–596.  
 [14] B. C. H. Steele, *Solid State Ionics* **2000**, *129*, 95–110.  
 [15] T. Hibino, A. Hashimoto, T. Inoue, J. Tokuno, S. Yoshida, M. Sano, *J. Electrochem. Soc.* **2000**, *147*, 2888–2892.  
 [16] T. Hibino, A. Hashimoto, M. Yano, M. Suzuki, S. Yoshida, M. Sano, *J. Electrochem. Soc.* **2002**, *149*, A133–A136.  
 [17] A. Tomita, S. Teranishi, M. Nagao, T. Hibino, M. Sano, *J. Electrochem. Soc.* **2006**, *153*, A956–A960.  
 [18] T. Suzuki, P. Jasinski, V. Petrovsky, H. U. Anderson, F. Dogan, *J. Electrochem. Soc.* **2005**, *152*, A527–A531.  
 [19] X. Jacques-Bedard, T. W. Napporn, R. Roberge, M. Meunier, *J. Power Sources* **2006**, *153*, 108–113.  
 [20] A. Y. Yan, M. J. Cheng, Y. L. Dong, W. S. Yang, V. Maragou, S. Q. Song, P. Tsiakaras, *Appl. Catal. B* **2006**, *66*, 64–71.